

RESEARCH PAPER

# Subcellular analysis of starch metabolism in developing barley seeds using a non-aqueous fractionation method

Axel Tiessen<sup>1,2,\*</sup>, Annika Nerlich<sup>3,\*</sup>, Benjamin Faix<sup>2</sup>, Christine Hümmer<sup>2</sup>, Simon Fox<sup>4</sup>, Kay Trafford<sup>4</sup>, Hans Weber<sup>5</sup>, Winfriede Weschke<sup>5</sup> and Peter Geigenberger<sup>2,†</sup>

<sup>1</sup> Departamento de Ingeniería Genética, CINVESTAV, Campus Guanajuato, 36821 Irapuato, México

<sup>2</sup> Ludwig-Maximilians-Universität München, Department Biologie I, Grosshaderner Str. 2–4, D-82152 Martinsried, Germany

<sup>3</sup> Max-Planck-Institut für Molekulare Pflanzenphysiologie, Am Mühlenberg 1, D-14476 Golm, Germany

<sup>4</sup> John Innes Centre, Norwich Research Park, Colney, Norwich, UK

<sup>5</sup> Leibniz-Institut für Pflanzengenetik und Kulturpflanzenforschung (IPK), D-06466 Gatersleben, Germany

\* These authors contributed equally to this work.

† To whom correspondence should be addressed. E-mail: [geigenberger@bio.lmu.de](mailto:geigenberger@bio.lmu.de)

Received 11 July 2011; Revised 17 November 2011; Accepted 21 November 2011

## Abstract

Compartmentation of metabolism in developing seeds is poorly understood due to the lack of data on metabolite distributions at the subcellular level. In this report, a non-aqueous fractionation method is described that allows subcellular concentrations of metabolites in developing barley endosperm to be calculated. (i) Analysis of subcellular volumes in developing endosperm using micrographs shows that plastids and cytosol occupy 50.5% and 49.9% of the total cell volume, respectively, while vacuoles and mitochondria can be neglected. (ii) By using non-aqueous fractionation, subcellular distribution between the cytosol and plastid of the levels of metabolites involved in sucrose degradation, starch synthesis, and respiration were determined. With the exception of ADP and AMP which were mainly located in the plastid, most other metabolites of carbon and energy metabolism were mainly located outside the plastid in the cytosolic compartment. (iii) In developing barley endosperm, the ultimate precursor of starch, ADPGlc, was mainly located in the cytosol (80–90%), which was opposite to the situation in growing potato tubers where ADPGlc was almost exclusively located in the plastid (98%). This reflects the different subcellular distribution of ADPGlc pyrophosphorylase (AGPase) in these tissues. (iv) Cytosolic concentrations of ADPGlc were found to be close to the published  $K_m$  values of AGPase and the ADPGlc/ADP transporter at the plastid envelope. Also the concentrations of the reaction partners glucose-1-phosphate, ATP, and inorganic pyrophosphate were close to the respective  $K_m$  values of AGPase. (v) Knock-out of cytosolic AGPase in *Riso16* mutants led to a strong decrease in ADPGlc level, in both the cytosol and plastid, whereas knock-down of the ADPGlc/ADP transporter led to a large shift in the intracellular distribution of ADPGlc. (vi) The thermodynamic structure of the pathway of sucrose to starch was determined by calculating the mass-action ratios of all the steps in the pathway. The data show that AGPase is close to equilibrium, in both the cytosol and plastid, whereas the ADPGlc/ADP transporter is strongly displaced from equilibrium *in vivo*. This is in contrast to most other tissues, including leaves and potato tubers. (vii) Results indicate transport rather than synthesis of ADPGlc to be the major regulatory site of starch synthesis in barley endosperm. The reversibility of AGPase in the plastid has important implications for the regulation of carbon partitioning between different biosynthetic pathways.

**Key words:** Cereal seeds, metabolic regulation, non-aqueous fractionation, starch, subcellular metabolite analysis.

## Introduction

Starch is of great importance both as a physiological and dynamic carbon storage reserve in higher plants and as a useful renewable raw material for human nutrition and industrial biotechnology (Geigenberger and Fernie, 2006;

Smith, 2008; Zeeman *et al.*, 2010). Starch from cereals feeds humanity, since maize, wheat, and rice account for 87% of all grain production, worldwide, and 43% of all food calories (FAO, 2003). Despite their great economic importance, there is still a lack of knowledge concerning the regulation of starch accumulation in cereal seeds (Geigenberger, 2011). While previous attempts to manipulate starch metabolism in this tissue were performed with limited success (Hannah and James, 2008), a much deeper knowledge of the regulation of the metabolic network will be required to manipulate metabolism in a more predictable way.

The conversion of sucrose to starch in storage tissues has been the subject of intense research in the past decades, leading to a good knowledge of the pathways and enzymes involved (James *et al.*, 2003; Geigenberger *et al.*, 2004; Tetlow *et al.*, 2004a; Geigenberger 2011). In most heterotrophic tissues (Fig. 1A), sucrose is mobilized by a series of reactions to glucose-6-phosphate (Glc6P), which is imported into the amyloplast in counter-exchange with inorganic phosphate (Pi) (Kammerer *et al.*, 1998) and converted to glucose-1-phosphate (Glc1P) via plastidial phosphoglucomutase (PGM). ATP is provided by mitochondrial respiration and imported into the plastid via the envelope ATP/ADP exchanger (Tjaden *et al.*, 1998; Geigenberger *et al.*, 2001). The conversion of Glc1P and ATP to ADP-glucose (ADPGlc) and inorganic pyrophosphate (PPi) is catalysed by ADPGlc-pyrophosphorylase (AGPase), which is located inside the plastid. The PPi produced in the AGPase reaction is hydrolysed to Pi by inorganic pyrophosphatase (Gross and apRees, 1986). ADPGlc acts as the glucosyl donor for different classes of starch synthases, which elongate the  $\alpha$ -glucan chains of amylose and amylopectin in coordinated action with branching and debranching enzymes that modify the fine structure of starch (Zeeman *et al.*, 2010).

The pathway of starch synthesis in cereal endosperm (Fig. 1B) is more complicated due to the additional presence of an AGPase in the cytosol that accounts for 85–95% of the total activity (James *et al.*, 2003). There is genetic and biochemical evidence that ADPGlc produced in the cytosol is subsequently transported into the plastid by the *brittle1*-encoded ADPGlc/ADP antiporter at the amyloplast envelope (Mangelsdorf and Jones, 1926; Shannon *et al.*, 1998; Bowsher *et al.*, 2007; Kirchberger *et al.*, 2007) to be used for starch synthesis. Although mutants of cytosolic AGPase and the *brittle1* ADPGlc/ADP transporter have been found to be deficient in starch accumulation (Jeon *et al.*, 2010), the importance of these two additional steps for the regulation of starch synthesis has not yet been fully resolved. Recent advances in understanding the regulation of this unique pathway in cereal endosperm were mainly focused on the role of reversible protein phosphorylation and protein complex formation of the plastidial enzymes. In maize and wheat, multienzyme complexes were found comprising specific isoforms of starch synthases and starch branching enzymes (Tetlow *et al.*, 2004b, 2008; Hennen-Bierwagen *et al.*, 2008). While there is evidence that complex formation depends on the phosphorylation status of some of its constituent enzymes (Tetlow *et al.*, 2004b; Liu *et al.*, 2009), the *in vivo* relevance and physiological importance of these

complexes for the regulation of starch synthesis are largely unresolved. Interestingly, pyruvate:phosphate dikinase (PPDK), not previously known to be integral to the pathway of plastidial starch synthesis, has been found to be associated with these complexes (Hennen-Bierwagen *et al.*, 2009). PPDK generates PPi, and it has been suggested that this enzyme leads to an increase in plastidial PPi concentrations affecting the catalytic direction of AGPase in the plastid (Hennen-Bierwagen *et al.*, 2009). Data on the plastidial concentrations of the reaction partners of PPDK and AGPase would be required to support this hypothesis.

More detailed and comprehensive analyses of metabolite profiles would also be needed to resolve fully the regulatory network of starch biosynthesis in the developing cereal endosperm. Up to now, there have been a few studies only of metabolite levels in this tissue, compared with transcript, protein, and enzyme studies. Moreover, this work is hampered by a lack of knowledge of the subcellular compartmentation of most of the metabolites involved in the conversion of sucrose to starch, specifically ADPGlc. Although techniques were developed in the past to measure subcellular metabolite levels in leaves (Stitt *et al.*, 1989) and potato tubers (Farre *et al.*, 2001; Tiessen, 2000; Tiessen *et al.*, 2002), they have not previously been employed successfully to allow similar extensive analyses in seeds.

The aim of the present work was to establish a non-aqueous fractionation (NAF) method that can be used to measure subcellular metabolite levels in the developing barley seed endosperm. By using this method, the cytosolic and plastidial levels of all the intermediates of the pathway of sucrose to starch conversion have been determined. Alterations in the subcellular levels of ADPGlc were analysed in barley mutants defective in cytosolic AGPase (*Riso16*; Johnson *et al.*, 2003) or the ADPGlc transporter (*Riso13*; Patron *et al.*, 2004), and for comparison also in growing potato tubers. The data were used to calculate *in vivo* mass-action ratios of all the reactions between sucrose and starch to pinpoint steps that are displaced from thermodynamic equilibrium, which are proposed to be important for regulation. Results have important implications for the understanding of starch metabolism in cereal seeds, showing that both cytosolic and plastidial AGPase are catalysing reversible reactions in the context of high PPi concentrations in the cytosol and plastid, and pinpointing intracellular transport of ADPGlc to be an important step for the regulation of starch synthesis and other plastidial pathways requiring carbon or ATP.

## Materials and methods

### Plant material

Plants from two-rowed spring barley (*Hordeum vulgare* cv. Bomi) were cultivated in pots, 18 cm in diameter, in a mixture of compost and sand. Fertilization was performed with Osmocote Pro 3-4M (<http://www.hauert.com/profibereich/baumschulen/osmocote.html>) with repetitions at 4–5 weeks. Growth conditions in greenhouses were 12–14 °C for 3 weeks and a light/dark regime of 11/13 h. During the generative phase, plants were grown at 18–20 °C and

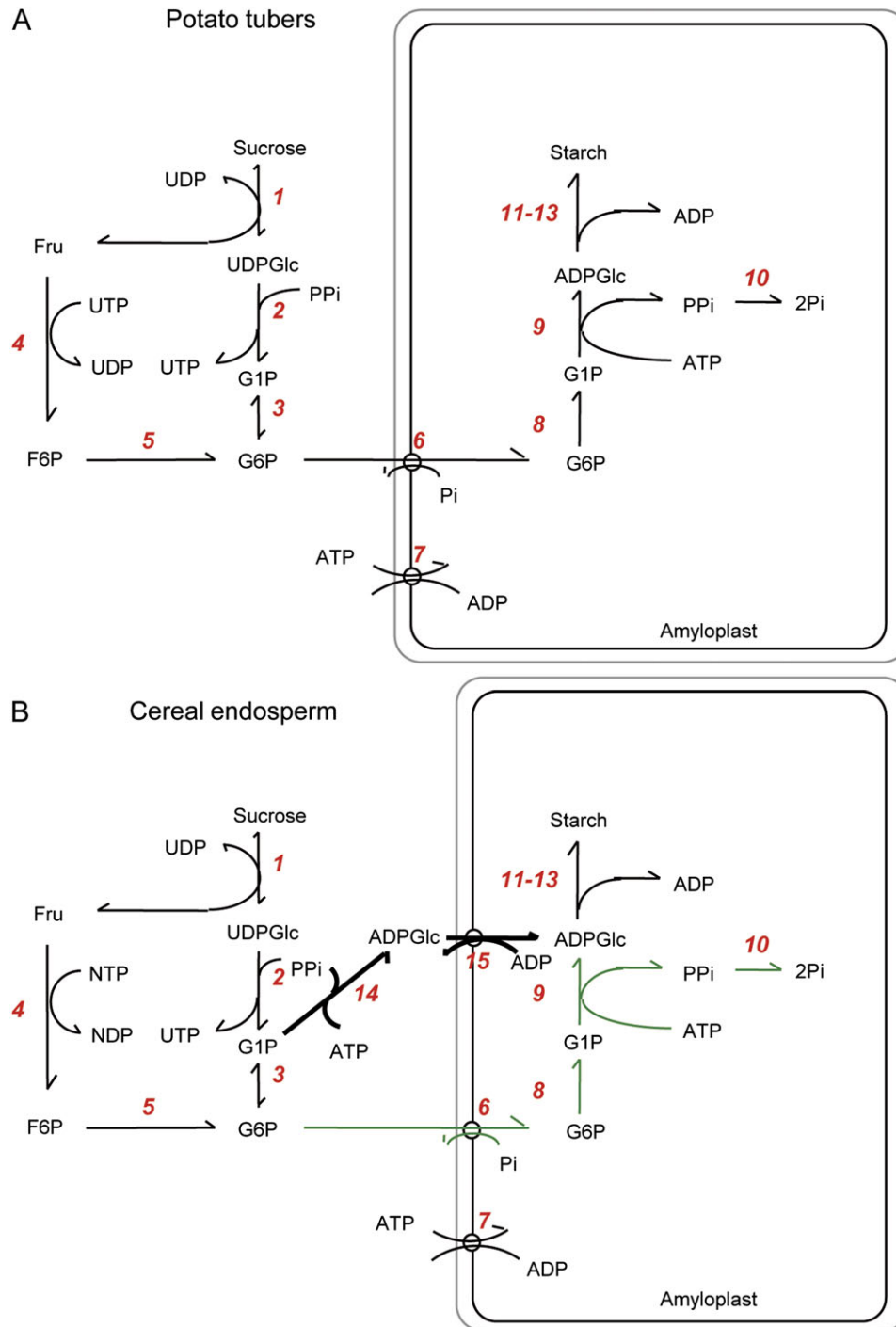


**Fig. 1.** Outline of the biochemical pathways of starch synthesis in heterotrophic tissues: (A) growing potato tubers and (B) developing cereal endosperm. The reactions are catalysed by the following enzymes: 1, sucrose synthase; 2, UDP-glucose pyrophosphorylase; 3, phosphoglucomutase (cytosol); 4, hexokinase; 5, phosphoglucoisomerase; 6, glucose-6-phosphate/Pi translocator; 7, ATP-ADP translocator; 8, phosphoglucomutase (plastid); 9, ADP-glucose pyrophosphorylase (plastid); 10, inorganic pyrophosphatase; 11, starch synthase; 12, starch branching enzyme; 13, starch debranching enzyme; 14, ADP-glucose pyrophosphorylase (cytosol); and 15, ADP-glucose/ADP translocator. Steps 14 and 15 are specific for cereal endosperm, providing an additional route of carbon entry into the amyloplast. (This figure is available in colour at *JXB* online.)

a light/dark regime of 17/7 h. Plants were flowering ~10–12 weeks after sowing. Days after flowering (DAF) were defined by determining anthesis on spikelets in the centre one-third of the spikes. Only five kernels from each row corresponding to this region were used in all the studies. At 14 DAF, endosperm tissue was harvested and snap-frozen in liquid nitrogen for further use.

#### *Histological method and microscopy*

Grains were harvested at 14 DAF and processed, fixed, and embedded as described in *Weschke et al.* (2000). Sections were made at 3  $\mu$ m using a Leica Rotationsmicrotom RM2265. Sections were then photographed with a Zeiss, Axioscop equipped with an AxioCam HRc. Only the middle part of the caryopses, which

optimally reflects the contents of endosperm cells, was chosen for sectioning. Fixation and embedding slightly change the volume of the caryopses, but this occurs in a uniform manner for the different tissues of the caryopses (Gubatz *et al.* 2007).

#### Determination of subcellular volumes

Over 90 different micrographs were used for the evaluation of subcellular volumes according to the principle of Delesse (1847): 'the areal density of profiles on sections is an unbiased estimate of the volume density of structures' (as described in Weibel and Bolender, 1973; Winter *et al.*, 1993; Farre *et al.*, 2001). More than 300 different cells were evaluated with respect to their plastidial and extraplastidial areas as a percentage of total cell area using ImageJ software (<http://rsbweb.nih.gov/ij/>).

#### Non-aqueous fractionation of seed material

The rationale of the NAF method is to separate different fractions of homogenized and lyophilized material in a density gradient formed with non-polar solvents (Gerhardt and Heldt, 1984; Stitt *et al.*, 1989). In order to obtain the distribution of metabolites in the different subcellular compartments one has to measure enzyme activities [e.g. UDP-glucose pyrophosphorylase (UGPase), alcohol dehydrogenase, starch synthase, sucrose synthase, alkaline pyrophosphatase] or metabolite levels (e.g. starch) that can be used reliably as markers. As in any fractionation method, the results depend heavily on the assumptions of the employed markers. The quantitative values of both metabolites and marker enzymes in each fraction are then used as variables within a previously defined mathematical model containing as many equations as fractions collected, and as many linear factorial elements as subcellular compartments analysed. The experimentally known values of the content of metabolites or markers are extrapolated to the unknown subcellular distribution values by a linear regression model. The best-fit solution can be obtained by the least squares method, and this is done practically using the solver add-in function incorporated into Microsoft Excel.

#### Preparation of subcellular particles of barley endosperm

Barley seed tissue was processed and fractionated using the basic procedures described previously for potato tubers (Farré *et al.*, 2001; Tiessen *et al.*, 2002) with some minor but significant adjustments or improvements. Developing barley endosperm (milky stage ~14 DAF) was frozen in liquid nitrogen and homogenized using an iron-ball swing mill (Retsch, Germany) pre-cooled with liquid nitrogen. The frozen powder [6 g fresh weight (FW); mean particle size ~50 µm] was transferred immediately to a 50 ml polypropylene tube (Falcon), resuspended in liquid nitrogen, and then freeze-dried (lyophilized at 4 Pa vacuum) for 4 d in a lyophilizer which had been pre-cooled to -40 °C. Lyophilization was completed when the temperature of the sample increased to room temperature levels for >1 d. The lyophilization procedure allowed metabolites and enzymes to be stable at room temperature (Farré *et al.*, 2001). During the whole procedure, special care was taken that the particles did not absorb humidity or water during the NAF. This was achieved by working at room temperature and in an environment of ~0% relative humidity, and using water-free organic solvents. Tetrachlorethylene (density=1.62 g ml<sup>-1</sup>) and *n*-heptane (density=0.68 g ml<sup>-1</sup>) (both from Merck, Uvasol quality) were treated and stored with 5 nm molecular sieves (Merck) to trap contaminating water molecules.

The lyophilized barley material (8 ml powder volume) was suspended in 20 ml of a tetrachlorethylene/heptane mixture (66:34, v/v; density=1.30 g ml<sup>-1</sup>). The particles were then ultrasonified to avoid clustering and to reduce particle size further (2 min sonification at full power with 50% time intervals using a Bandolin Sonoplus HD 200, MS 73/D). To prevent overheating, the polypropylene tube was placed on an aluminium block pre-

cooled at -20 °C. The particles were filtered first through a 100 µm nylon net and then through a 30 µm nylon net, washed with 20 ml of heptane, and collected in a 50 ml tube and then centrifuged at 10 000 g for 10 min. The pellet was re-suspended in 4 ml of tetrachlorethylene/heptane mixture (66:34, v/v). Four 0.5 ml aliquots of this initial homogenate (total aliquots) were taken to determine total enzyme activities and metabolites loaded onto the gradient. These aliquots were used to determine total dry weight (~0.8 g DW per gradient) and to calculate the recovery values of enzymes and metabolites for each gradient. Recovery values for barley endosperm usually ranged from 85% to 110% (data not shown).

#### Density gradient and fractionation of barley endosperm

The gradient was formed in a 50 ml polypropylene tube (Falcon) with the help of a metallic needle (1.5 mm diameter and 20 cm long) and a peristaltic pump (BioRad gradient pump) with silicon tubing. A 3 ml aliquot of the particle homogenate was followed by 35 ml of a linear gradient from 100% solution A (66:34, v/v, tetrachlorethylene/heptane mixture) to 100% solution B (100% tetrachlorethylene), resulting in a density gradient from 1.30 g ml<sup>-1</sup> to 1.62 g ml<sup>-1</sup>. The gradient was centrifuged at 4000 rpm (RCF<sub>min</sub> 4000 g, RCF<sub>max</sub> 10 000 g) for 1 h in a swing-out rotor (Eppendorf) at 7 °C with minimum acceleration and deceleration (brakes off).

Five different fractions (termed 0, 1, 2, 3, and 4) were collected manually with a 1 ml cut pipette tip into 15 ml Falcon tubes and then filled up with heptane to a volume of 14 ml. Two 1.8 ml aliquots off each fraction were taken for marker enzyme measurements and the remaining 10.4 ml were used for metabolite analysis. Samples were centrifuged for 10 min at maximal speed, the organic solvent supernatant discarded, and the pellet dried at room temperature inside an excicator connected to a teflon-membrane vacuum pump (KNF Laboport) for 20 h. The dried fractions were stored at -20 °C in plastic bags containing silica gel until further processing. The mass of the dried total aliquot was used to express the results per g of DW.

The most prominent difference to the fractionation of potato tubers was that in the barley gradients the pellet and lowest fraction (termed p and 0) were usually particle free.

#### Enzyme assays

The aliquots of the dried fractions were re-suspended at 4 °C in 1000 µl of protein extraction buffer [50 mM HEPES-KOH pH 7.4, 5 mM MgCl<sub>2</sub>, 1 mM EDTA, 1 mM EGTA, 5 mM dithiothreitol (DTT), 2 mM benzamidine, 2 mM α-aminocaproic acid, 0.5 mM phenylmethylsulphonyl fluoride (PMSF), and 10% (v/v) glycerol]. The extract was centrifuged (10 000 g for 10 min at 4 °C) and the supernatant was used directly for the following enzymatic assays without prior freezing. Recoveries of enzyme activities during NAF have been documented previously (Stitt *et al.*, 1989).

AGPase was not used as marker enzyme, but its subcellular distribution was calculated from the other marker enzymes. The activity was assayed in the pyrophosphorolysis (reverse) direction in a coupled enzymatic assay and the absorbance measured at 340 nm (adapted from Tiessen *et al.*, 2002). The assay was carried out in a total volume of 200 µl containing 80 mM HEPES-KOH pH 7.4, 10 mM MgCl<sub>2</sub>, 10 µM glucose-1,6-bisphosphate, 10 mM 3-phosphoglyceric acid, 3 mM DTT, 0.6 mM NADP<sup>+</sup>, 0.6 mM ADP-glucose, 1 U ml<sup>-1</sup> PGM (from rabbit muscle), 2.5 U ml<sup>-1</sup> glucose-6-phosphate dehydrogenase (from yeast), and 20 µl of extract. The reaction was started by addition of 2 mM Na-PPi.

UGPase was used as one of the markers for the cytosol. UGPase activity was assayed in the pyrophosphorolysis direction in a coupled enzymatic assay and absorbance was measured at 340 nm (adapted from Geigenberger *et al.*, 1993). The assay was carried out in a total volume of 300 µl containing 100 mM TRIS-HCl pH 8, 2 mM MgCl<sub>2</sub>, 20 µM glucose-1,6-bisphosphate, 0.25 mM NADP<sup>+</sup>, 2 mM UDP glucose, 3 U ml<sup>-1</sup> PGM (from

rabbit muscle), 2.5 U ml<sup>-1</sup> glucose-6-phosphate dehydrogenase (from yeast), and 5 µl of extract. The reaction was started by addition of 2 mM Na-PPi.

α-Mannosidase was used as a vacuolar marker enzyme. The stop-assay (adapted from Stitt *et al.*, 1989) was carried out in 100 µl of 50 mM citrate pH 4.5 and 25 µl of extract, and started by addition of 25 µl of 5 mM *p*-nitrophenyl-D-α-mannoside. After an incubation of 30 min at 25 °C, the reaction was stopped by adding 150 µl of 1 M borate buffer pH 9 and the absorbance was measured at 405 nm after 5 min. Reaction blanks were stopped immediately with borate buffer without any incubation.

Other marker enzymes were measured as described elsewhere: sucrose synthase (Merlo *et al.*, 1993), alcohol dehydrogenase (Zabalza *et al.*, 2009), starch synthase (Jenner *et al.*, 1994; Burton *et al.*, 2002), and alkaline pyrophosphatase (Patron *et al.*, 2004). Total proteins were quantified via the Bradford method using a commercial reagent (BioRad) (Bradford, 1976).

#### Determination of metabolites

Metabolites were extracted using trichloroacetic acid (TCA) as described in Trethewey *et al.* (1998). With the exception of nucleotides which were measured by HPLC (Geigenberger *et al.*, 1997), all other metabolites were measured via enzyme-coupled spectrophotometric assays as described in Stitt *et al.* (1982, 1989) and Geigenberger *et al.* (1993). The reliability of the TCA extraction and assay protocol has been confirmed previously using recovery experiments (see Trethewey *et al.*, 1998; Farre *et al.* 2001).

#### Mathematical analysis of fractionation data

From the primary data, the corresponding subcellular compartmentation of AGPase or the metabolites was calculated by a quadratic best fit method (method of least squares values) using a specifically developed algorithm (Tiessen, 2000; Tiessen *et al.*, 2002) based on the solver function incorporated into the Excel program (Microsoft). All results were primarily calculated per fraction, or secondarily as the percentage found in all fractions or per g of DW.

The Excel sheets allowed direct calculation and evaluation of each gradient individually, considering the recovery values (% of total aliquot) and using percentage values (% of total found in all fractions) of marker enzymes and metabolites to make the linear regressions for subcellular compartments. The manual inspection of individual fractions in Excel allowed more efficient detection of analytic errors than earlier methods (Stitt *et al.*, 1989; Riens *et al.*, 1991; Farre *et al.*, 2001). By using a higher number of fractions (five plus one total aliquot) than the number of analysed compartments (two: plastid and non-plastid), the equation system is overdetermined, making the results on subcellular distribution more reliable and robust. Even when the data for one fraction are deleted or ignored, the linear regression model (solver function) can sometimes still give consistent values (data not shown).

The non-aqueous density gradient of barley endosperm resulted in partial enrichment of plastidial and cytosolic material (see Fig. 4). In contrast to potato tuber gradients, there was no significant enrichment of vacuolar material.

## Results

### Microscopic analysis of the developing barley endosperm and estimation of subcellular volumes

To determine the volumes of the different subcellular compartments, 90 micrographs were taken from representative regions of the developing barley endosperm at 14 DAF. From these photographs, the relative volumes of the plastid and extraplastid compartments (percentage of total) were calculated according to the principle of Delesse (1847) and are shown in Fig. 2. In the developing endosperm, the relative volume distribution was 50.5% for plastids and 49.5% for the extraplastidial compartment. The latter was mainly comprised of the cytosol. In all of the micrographs analysed, vacuoles were undetectable, showing that this

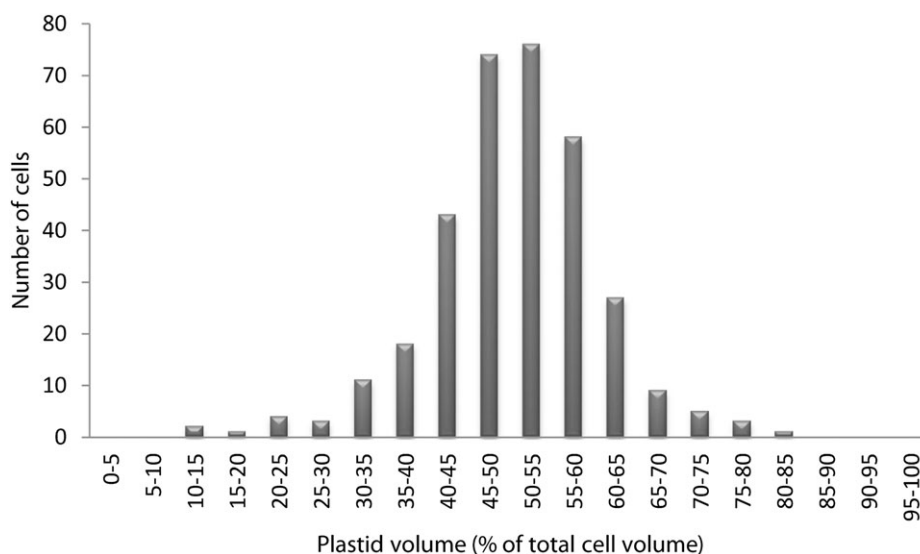


**Fig. 2.** Volume distribution of the plastidial compartment in developing barley endosperm. Ninety different cellular sections of developing barley endosperm (14 DAF) were visualized by microscopy. From these micrographs the relative plastidial volumes as a percentage of the total cell volume were calculated according to the principle of Delesse (1847). A total of 335 cells were analysed. The histogram of relative volume distribution shows the range of volumes obtained for the plastidial compartment. The mean value  $\pm$ SE is  $50.5 \pm 0.5$  for the plastidial and  $49.5 \pm 0.5$  for the extraplastidial compartment, respectively ( $n=335$ ). The extraplastidial compartment consists mainly of cytosol.

tissue is very poorly vacuolated or lacking vacuoles entirely. This differs from the subcellular volume distributions of most other plant tissues, where >70% of the total cell volume is usually occupied by vacuoles (see Winter *et al.*, 1993 for barley leaves; Leidreiter *et al.*, 1995 for potato leaves; Farre *et al.*, 2001 for potato tubers).

#### Separation of seed material from barley into subcellular compartments

To analyse the subcellular distribution of all the metabolites in the pathway of sucrose to starch conversion in developing barley endosperm, an NAF method was selected that had been initially developed for leaves (Gerhardt and Heldt, 1984; Stitt *et al.*, 1989; Heineke *et al.*, 1997; Fettke *et al.*, 2005), then adapted for tubers (Farre *et al.*, 2001; Tiessen *et al.*, 2002), and now for seeds. The principle of this method is the separation of lyophilized tissue particles in an organic solvent due to differences in particle density. Particle density is determined by the type of molecules that are present (mineral salts, proteins, carbohydrates, etc.), and, in the absence of water, this composition is usually characteristic of a specific subcellular compartment. The size of the particles applied to the fractionation gradient ideally should be as small as possible to reduce the possibility of including material from different organelles. The water-free environment ensures inactivation of all biological and biochemical activity and the avoidance of metabolite–enzyme redistribution during the separation procedure. See the Materials and methods section for a detailed description of the NAF procedure used for developing barley seeds. To describe it here briefly, developing endosperm tissue rapidly frozen in liquid nitrogen was used. Plant material was carefully lyophilized for >4 d in order to eliminate all residual moisture and matrix-bound water. Homogenized tissue was

re-suspended in a water-free tetrachlorethylene/*n*-heptane mixture [66/34 (v/v), density 1.30 g ml<sup>-1</sup>]. Particle size and clustering were minimized by ultrasound sonication and filtering to achieve a particle size <30 μm. Large amounts of lyophilized and homogenized tissue (>8 g DW) were prepared of each replicate sample in order to obtain enough material for gradient fraction separation and all downstream measurements. The material was separated on a linear gradient using *n*-heptane and tetrachlorethylene as non-aqueous solvents. Collected fractions were diluted with *n*-heptane and then divided into a small aliquot for analysis of marker enzymes and a large aliquot for analysis of metabolite levels. Rather than obtaining pure fractions, the NAF method relies on relative enrichment of subcellular particles. The data on marker enzyme and metabolite distribution of the differently enriched fractions have to be used for calculating subcellular distributions using linear regression models optimized by the least squares method.

AGPase has been used as a plastidial marker enzyme in previous reports on NAF of leaves and tubers (Gerhardt and Heldt, 1984; Gerhardt *et al.*, 1987; Leidreiter *et al.*, 1995; Tiessen, 2000; Farre *et al.*, 2001; Tiessen *et al.*, 2002; Fettke *et al.*, 2005; Geigenberger *et al.*, 2011). Since cereal endosperm is characterized by a distinctive subcellular compartmentation of AGPase, additional metabolites and enzymes were therefore measured as markers for the plastidial compartment, such as starch, soluble starch synthase, and inorganic pyrophosphatase. UGPase, sucrose synthase, and alcohol dehydrogenase were used as cytosolic markers, while mannosidase was used as a vacuolar marker. As shown in Fig. 3, fraction 0 is enriched for plastidial markers, whereas fractions 2, 3, and 4 rather are enriched for cytosolic markers. No enrichment of the vacuolar marker was obtained relative

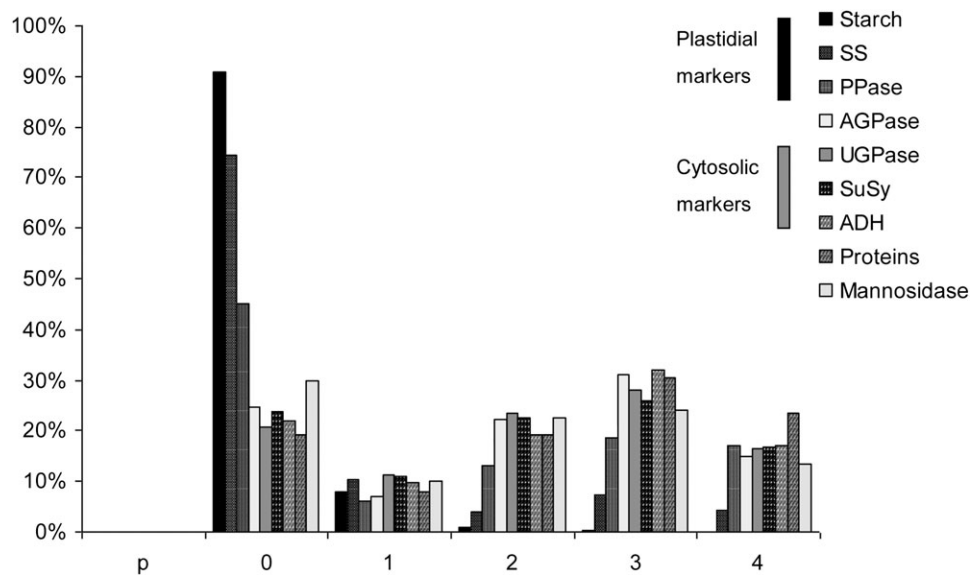


**Fig. 3.** Distribution of starch, enzymes, and proteins in a representative non-aqueous gradient prepared from developing barley seeds. The components that were used as markers for the plastidial compartment were starch, soluble starch synthase, and inorganic pyrophosphatase, while UDP-glucose pyrophosphorylase, sucrose synthase, and alcohol dehydrogenase were chosen as cytosolic markers, and mannosidase was used as a vacuolar marker. ADP-glucose pyrophosphorylase was also measured but not used as a marker. The bars give average values as a percentage of that total found in the gradient (sum of all fractions).

to the cytosolic markers. Therefore, only two subcellular compartments could be discriminated in the barley gradients: the plastidial and the cytosolic compartments.

The failure to discriminate the vacuolar compartment in barley endosperm is in contrast to the results obtained in potato tubers, where vacuolar, cytosolic, and plastidic particles could be enriched in different fractions (see comparison between barley seeds and potato tubers in Fig. 4). Obviously, vacuoles from tuber and endosperm tissues are very different in size, being undetectable in a large number of micrographs from developing barley endosperm (Fig. 2), while yielding >70% of the cell volume in potato tubers (Farre *et al.*, 2001). Therefore, it will be more difficult to separate vacuoles from the cytosolic surroundings in endosperm tissue, compared with potato tubers. While in potato the vacuolar particles were mainly found in the pellet fraction, this fraction was essentially free of subcellular particles in the barley gradients (Fig. 4). Based on the assumption that vacuolar particles from barley endosperm and potato show a similar distribution pattern during density gradient fractionation, this would indicate that vacuolar particles are not detectable in the barley gradients. Alternatively, vacuoles from barley endosperm might differ from those from potato tubers in containing smaller amounts of high density molecules such as oxalic crystals and mineral salts, leading to a distribution during fractionation similar to that of cytosolic particles.

The distribution of AGPase activity in the barley gradients resembled the cytosolic markers, rather than the plastidial markers (see Fig. 3). When calculated using the distribution of the given marker enzymes, 99% of the AGPase activity was assigned to the cytosol, whereas only 1% was found in the plastid. This is in line with previous studies in cereal endosperm showing that the activity of the cytosolic AGPase predominates over the plastidial isoform (James *et al.*, 2003).

#### *Analysis of subcellular metabolite levels and concentrations in the developing barley endosperm*

Subcellular metabolite distribution was calculated using the distribution of the given marker enzymes (see Fig. 4) by the method of linear regression with least square sums. Three different gradients were used to calculate the percentage subcellular distribution of metabolite levels between the cytosol and plastid (Table 1). With the exception of ADP and AMP which were mainly located in the plastid, most of the other metabolites were preferentially located outside the plastid in the cytosolic compartment. A total of 80–90% of the uridine nucleotides (UDPGlc, UTP, UDP, and UMP), ATP, GTP, PPi, and Pi were located in the cytosol, >90% of sucrose, fructose-1,6-bisphosphate, triose-phosphates, and intermediates of the citric acid cycle (citrate, isocitrate,  $\alpha$ -ketoglutarate, and malate) were also in the cytosol. There were clear differences in the energy status between these two compartments, with the ATP/ADP ratio and the adenylate energy charge [ATP+0.5ADP/(ATP+ADP+AMP)] of the plastid (0.35 and 0.44, respectively) being much lower than that of the cytosol (4.9 and 0.77, respectively). These results are consistent with data from leaves and potato tubers (Stitt

*et al.*, 1989; Farre *et al.*, 2001), showing that there is a similar trend in the subcellular distribution of the energy charge and of most of the metabolites in primary metabolism across different plant tissues. The absolute value of the cytosolic energy status in developing barley endosperm is lower than that in leaves, which is consistent with the occurrence of low internal oxygen concentrations in developing seed endosperm (van Dongen *et al.*, 2004)

The immediate precursor of starch synthesis, ADPGlc, was mainly located in the cytosol (~90%), rather than the plastid (Table 1). This provides direct biochemical evidence that ADPGlc formation and starch synthesis occur in different subcellular compartments. As expected from previous work, the majority of ADPGlc is formed in the cytosol and has to be transported into the plastid where starch synthesis takes place. As in other experiments, most of the AGPase activity in barley endosperm was found in the cytosol rather than the plastid (see above).

Subcellular metabolite levels in the cytosol and plastid (as nmol g FW<sup>-1</sup>) were calculated by multiplying the original tissue content by the percentage subcellular distribution of the respective metabolite for each gradient separately (Table 1). The obtained values for cytosolic and plastidial metabolite levels from the different gradients were then used to calculate the mean  $\pm$ SE ( $n=3$  different gradients). To calculate the subcellular concentration (in  $\mu$ M), the mean subcellular metabolite level was divided by the mean value of the percentage distribution of the respective subcellular volume (see Fig. 2). In this case, both the relative error of the respective metabolite level and that of the subcellular volume distribution were added to show the limits of variation (Table 1). The calculations of plastidial concentrations were performed assuming unrestricted diffusion of metabolites in the starch granule (see Farre *et al.*, 2001 for a more detailed discussion of this point). The cytosolic concentrations of sucrose, UDP, fructose, and UDPGlc (Table 1) were similar to the respective  $K_m$  values of sucrose synthase for these reaction partners (see Avigad, 1982), which is in line with sucrose synthase catalysing a readily reversible reaction in the developing barley endosperm (see also below). Interestingly, there were also substantial concentrations of sucrose (13 mM), UDP (0.02 mM), UDPGlc (0.05 mM), and fructose (0.87 mM) in the plastid, indicating an unexpected role for sucrose metabolism in this compartment (Table 1). It is also known that these metabolites are present in small amounts inside potato tuber amyloplasts (Tiessen, 2000; Farre *et al.*, 2001). However, it is believed that sucrose synthase does not play a major role inside the plastid since measurements of enzyme activities in the non-aqueous barley gradients confirmed that sucrose synthase has a similar distribution pattern to that of other cytosolic marker enzymes, such as UGPase and alcohol dehydrogenase (Fig. 3). While this indicates that the majority of sucrose synthase is located in the cytosol, it cannot be excluded that some sucrose synthase activity is also present in the plastid and equilibrates plastidial metabolites directly. Alternatively, cytosolic sucrose synthase might influence plastidial metabolism in an indirect manner if metabolites

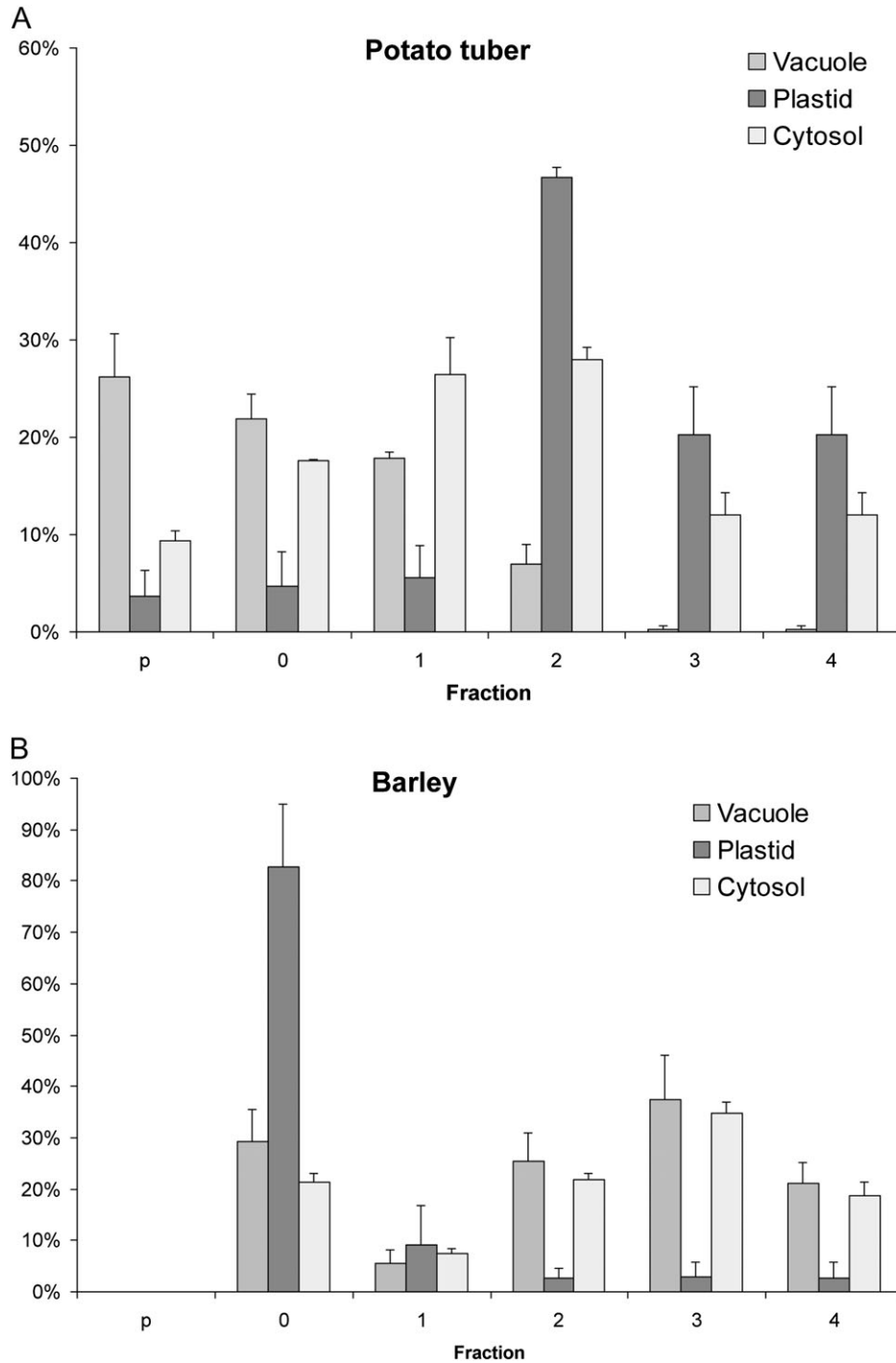


**Fig. 4.** Distribution of various subcellular compartments in different fractions of a non-aqueous gradient from potato tuber (A) or developing barley endosperm (B). The plastid is enriched in fraction 2 of the potato gradient, or in fraction 0 of the barley gradient. Whereas in potato it was possible to obtain different ratios of vacuolar to cytosolic particles in all fractions, in the barley gradient the distribution of vacuolar particles was not significantly different from that of the cytosolic particles. Bars represent means  $\pm$ SE of the selected set of markers ( $n=3-4$ ) for potato or barley.

could diffuse through the plastidial membrane or are co-transported non-specifically (Angeles-Nuñez and Tiessen, 2010).

There were also significant concentrations of ATP (66  $\mu$ M), pyruvate (26  $\mu$ M), Pi (6520  $\mu$ M), AMP (109  $\mu$ M), PEP (11  $\mu$ M), and PPi (18  $\mu$ M) in the plastid (Table 1), that

were close to the  $K_{ms}$  of maize PPK for these reaction partners (15, 250, 1500, 10, 40, and 140  $\mu$ M, respectively; Sugiyama, 1973). This suggests that PPK will be able to catalyse a readily reversible reaction in the plastid, in the direction of the synthesis of ATP, pyruvate, and Pi, as well as in the direction of AMP, PEP, and PPi synthesis.

**Table 1.** Subcellular distribution of metabolite levels in developing barley endosperm tissue at 14 DAF

For three separate gradients deriving from the same pool of tissue, the percentage subcellular distribution of the respective metabolite was calculated. The data shown are the mean  $\pm$ SE ( $n=3$  different gradients). The levels of the respective metabolite ( $\text{nmol g FW}^{-1}$ ) in cytosol and plastid were calculated by multiplying the tissue content by the percentage subcellular distribution of the respective metabolite for each gradient separately. The obtained values for cytosolic and plastidial metabolite levels from the different gradients were then used to calculate the mean  $\pm$ SE ( $n=3$  different gradients).

Metabolite	Tissue content ( $\text{nmol g FW}^{-1}$ )	Subcellular distribution (%)		Subcellular levels ( $\text{nmol g FW}^{-1}$ )		Subcellular concentrations ( $\mu\text{M}$ )	
		Cytosol	Plastid	Cytosol	Plastid	Cytosol	Plastid
Sucrose	75 000.0	91.2 $\pm$ 2.9	8.8 $\pm$ 2.9	68 432.9 $\pm$ 2209.4	6603.2 $\pm$ 2209.4	138.248 $\pm$ 5.860	13.076 $\pm$ 4.505
Fructose	2500.0	82.2 $\pm$ 2.7	17.8 $\pm$ 2.7	2024.5 $\pm$ 65.4	438.4 $\pm$ 65.4	4.090 $\pm$ 0.173	0.868 $\pm$ 0.138
Gluc-1-P	42.2	85.2 $\pm$ 5.4	14.8 $\pm$ 5.4	36.0 $\pm$ 2.3	6.3 $\pm$ 2.3	0.073 $\pm$ 0.005	0.012 $\pm$ 0.005
Gluc-6-P	686.6	87.5 $\pm$ 4.2	12.5 $\pm$ 4.2	600.7 $\pm$ 28.5	85.8 $\pm$ 28.5	1.214 $\pm$ 0.070	0.170 $\pm$ 0.058
Fruc-6-P	152.1	75.5 $\pm$ 5.0	24.5 $\pm$ 5.0	114.8 $\pm$ 7.6	37.3 $\pm$ 7.6	0.232 $\pm$ 0.018	0.074 $\pm$ 0.016
Fruc-1,6-bisP	23.5	91.5 $\pm$ 2.3	8.5 $\pm$ 2.3	21.5 $\pm$ 0.5	2.0 $\pm$ 0.5	0.044 $\pm$ 0.002	0.004 $\pm$ 0.001
DHAP	31.7	95.5 $\pm$ 0.0	4.5 $\pm$ 0.0	30.3 $\pm$ 0.0	1.4 $\pm$ 0.0	0.061 $\pm$ 0.001	0.003 $\pm$ 0.000
GAP	12.8	98.0 $\pm$ 0.0	2.0 $\pm$ 0.0	12.5 $\pm$ 0.0	0.3 $\pm$ 0.0	0.025 $\pm$ 0.000	0.001 $\pm$ 0.000
3-PGA	277.5	85.8 $\pm$ 5.3	14.2 $\pm$ 5.3	238.1 $\pm$ 14.6	39.4 $\pm$ 14.6	0.481 $\pm$ 0.034	0.078 $\pm$ 0.030
PEP	43.7	87.8 $\pm$ 0.9	12.2 $\pm$ 0.9	38.4 $\pm$ 0.4	5.3 $\pm$ 0.4	0.078 $\pm$ 0.002	0.011 $\pm$ 0.001
Pyruvate	61.9	78.8 $\pm$ 5.2	21.2 $\pm$ 5.2	48.8 $\pm$ 3.2	13.1 $\pm$ 3.2	0.099 $\pm$ 0.007	0.026 $\pm$ 0.007
Citrate	1805.2	91.2 $\pm$ 4.3	8.8 $\pm$ 4.3	1646.3 $\pm$ 78.2	158.9 $\pm$ 78.2	3.326 $\pm$ 0.192	0.315 $\pm$ 0.158
Isocitrate	260.0	91.8 $\pm$ 3.7	8.2 $\pm$ 3.7	238.7 $\pm$ 9.6	21.3 $\pm$ 9.6	0.482 $\pm$ 0.024	0.042 $\pm$ 0.019
Oxoglutarate	148.0	93.8 $\pm$ 1.7	6.2 $\pm$ 1.7	138.8 $\pm$ 2.5	9.2 $\pm$ 2.5	0.280 $\pm$ 0.008	0.018 $\pm$ 0.005
Malate	406.3	91.2 $\pm$ 2.6	8.8 $\pm$ 2.6	370.5 $\pm$ 10.6	35.8 $\pm$ 10.6	0.749 $\pm$ 0.029	0.071 $\pm$ 0.022
ADPG	146.0	91.0 $\pm$ 2.7	9.0 $\pm$ 2.7	132.9 $\pm$ 3.9	13.1 $\pm$ 3.9	0.268 $\pm$ 0.011	0.026 $\pm$ 0.008
ATP	258.9	87.2 $\pm$ 3.5	12.8 $\pm$ 3.5	225.8 $\pm$ 9.1	33.1 $\pm$ 9.1	0.456 $\pm$ 0.023	0.066 $\pm$ 0.019
ADP	139.2	33.0 $\pm$ 2.9	67.0 $\pm$ 2.9	45.9 $\pm$ 4.0	93.3 $\pm$ 4.0	0.093 $\pm$ 0.009	0.185 $\pm$ 0.010
AMP	103.4	46.7 $\pm$ 5.0	53.3 $\pm$ 5.0	48.3 $\pm$ 5.1	55.1 $\pm$ 5.1	0.098 $\pm$ 0.011	0.109 $\pm$ 0.011
UDPG	190.9	86.5 $\pm$ 2.7	13.5 $\pm$ 2.7	165.1 $\pm$ 5.1	25.8 $\pm$ 5.1	0.334 $\pm$ 0.014	0.051 $\pm$ 0.011
UTP	120.3	94.2 $\pm$ 1.3	5.8 $\pm$ 1.3	113.3 $\pm$ 1.6	7.0 $\pm$ 1.6	0.229 $\pm$ 0.006	0.014 $\pm$ 0.003
UDP	52.8	83.3 $\pm$ 2.7	16.7 $\pm$ 2.7	44.0 $\pm$ 1.4	8.8 $\pm$ 1.4	0.089 $\pm$ 0.004	0.017 $\pm$ 0.003
UMP	59.6	85.2 $\pm$ 2.3	14.8 $\pm$ 2.3	50.8 $\pm$ 1.4	8.8 $\pm$ 1.4	0.103 $\pm$ 0.004	0.017 $\pm$ 0.003
GTP	91.3	92.8 $\pm$ 2.7	7.2 $\pm$ 2.7	84.8 $\pm$ 2.4	6.6 $\pm$ 2.4	0.171 $\pm$ 0.007	0.013 $\pm$ 0.005
GDP	42.8	93.2 $\pm$ 2.3	6.8 $\pm$ 2.3	39.9 $\pm$ 1.0	2.9 $\pm$ 1.0	0.081 $\pm$ 0.003	0.006 $\pm$ 0.002
GMP	27.9	70.2 $\pm$ 4.9	29.8 $\pm$ 4.9	19.6 $\pm$ 1.4	8.3 $\pm$ 1.4	0.040 $\pm$ 0.003	0.016 $\pm$ 0.003
PPi	70.7	86.8 $\pm$ 4.7	13.2 $\pm$ 4.7	61.4 $\pm$ 3.3	9.3 $\pm$ 3.3	0.124 $\pm$ 0.008	0.018 $\pm$ 0.007
Pi	16 600.0	80.2 $\pm$ 4.4	19.8 $\pm$ 4.4	13 337.1 $\pm$ 729.7	3292.7 $\pm$ 729.7	26.944 $\pm$ 1.746	6.520 $\pm$ 1.509

To calculate the subcellular concentration (in  $\mu\text{M}$ ), the mean subcellular metabolite level was divided by the mean value of the percentage distribution of the respective subcellular volume (see Fig. 2). In this case, both the relative error of the respective metabolite level and that of the subcellular volume distribution were added to show the limits of variation. Cytosol also includes minor contributions of mitochondria and vacuoles that could not be further separated. Data are the mean  $\pm$ SE ( $n=3$  different experiments).

The cytosolic concentrations of the reaction partners of AGPase (Table 1), Glc1P (73  $\mu\text{M}$ ), ATP (456  $\mu\text{M}$ ), ADPGlc (268  $\mu\text{M}$ ), and PPi (124  $\mu\text{M}$ ), were similar to the respective  $K_m$  values of AGPase from barley endosperm, yielding 120, 310, 140, and 35  $\mu\text{M}$ , respectively (Doan *et al.*, 1999). This is consistent with AGPase having the potential to catalyse the forward and reverse reactions at similar rates *in vivo*. The results also suggest that AGPase is able to maintain relatively high concentrations of ADPGlc in the cytosol (268  $\mu\text{M}$ ), which are close to the  $K_m$  (ADPGlc) of the maize *brittle1* ADPGlc transporter (850  $\mu\text{M}$ ) that is known to have a relatively low affinity for ADPGlc (Kirchberger *et al.*, 2007). The concentration of ADP in the plastid (185  $\mu\text{M}$ ) is also close to the  $K_m$  (ADP) of the *brittle1* transporter (465  $\mu\text{M}$ ; Kirchberger *et al.*, 2007). There are large concentration gradients between the cytosol

and plastid of ADPGlc (268  $\mu\text{M}$  and 26  $\mu\text{M}$ , respectively) and ADP (93  $\mu\text{M}$  and 185  $\mu\text{M}$ , respectively), which would favour uptake of ADPGlc into the plastid in counter-exchange with ADP (Table 1).

#### Subcellular analysis of ADPGlc levels in barley mutants defective in genes involved in synthesis and intracellular transport of ADPGlc

To investigate the factors influencing the distribution of ADPGlc between the cytosol and plastid in developing barley endosperm, mutants defective in genes involved in the synthesis and intracellular transport of ADPGlc were analysed. In wild-type barley seeds,  $\sim 80\%$  of the ADPGlc was located in the cytosol (Table 2), confirming the results presented in the experiments above (compare Table 2 with

**Table 2.** Subcellular distribution of ADPGlc in the developing endosperm of barley mutants *Riso16* and *Riso13*, compared with barley wild type (*Bomi*) and growing potato tubers

The *Riso13* mutant is defective in the *brittle1* gene, coding for the ADPGlc transporter, while the *Riso16* mutant is defective in cytosolic AGPase. In barley, the ADPGlc levels (nmol g DW<sup>-1</sup>) in the cytosol and plastid were calculated by multiplying the total tissue content by the percentage subcellular distribution of the respective metabolite for each gradient separately. The obtained values for cytosolic and plastidial ADPGlc levels from three different gradients were then used to calculate the mean  $\pm$ SE and to perform statistics using the *t*-test.

Genotype	ADPGlc (nmol g DW <sup>-1</sup> )		ADPGlc (% of total)		ADPGlc ( $\mu$ M)	
	Cytosol	Plastid	Cytosol	Plastid	Cytosol	Plastid
Bomi wild type	234 $\pm$ 17	73 $\pm$ 17	76	24	236	72
Barley <i>Riso16</i>	59 $\pm$ 9*	11 $\pm$ 9*	84	16	60	11
Barley <i>Riso13</i>	4747 $\pm$ 891*	1 $\pm$ 10*	100	0	4795	1
Potato tubers	0.35 $\pm$ 0.30*	16.1 $\pm$ 1.4*	2.1	97.9	0.4	21.6

To calculate the concentration (in  $\mu$ M), the mean ADPGlc level on a FW basis was divided by the mean value of the percentage distribution of the respective subcellular volume (see Fig. 2). Subcellular levels of ADPGlc in growing potato tubers were also analysed and are shown for comparison. The subcellular concentrations for growing potato tubers were calculated as in Tiessen *et al.* (2002). The cytosol also includes minor contributions of mitochondria (potato tubers) or mitochondria plus vacuoles (barley endosperm) that could not be further separated. Values that are significantly different from Bomi wild type are indicated with asterisks ( $P < 0.05$  using Student's *t*-test)

Table 1). The data from Tables 1 and 2 derive from plants growing in different trials, which might explain the small differences between the values presented. Compared with the wild type, the *Riso16* mutant that is defective in cytosolic AGPase (Johnson *et al.*, 2003) showed a strong and significant decrease in ADPGlc content, in both the cytosol and plastid (Table 2). In the *Riso13* mutant, that is defective in the *brittle1* homologue coding for a plastidial ADPGlc transporter (Patron *et al.*, 2004), both the overall level and the subcellular distribution of ADPGlc were severely and significantly altered, compared with the wild type (Table 2). ADPGlc increased >20-fold in the cytosol, while it decreased below the detection limit in the plastid. Obviously, the *brittle1* protein is responsible for most, if not all of the intracellular transport of ADPGlc between both compartments. Overall, the results provide genetic evidence that the plastidial levels of ADPGlc in the wild type are mainly determined by the import and provision of ADPGlc from the cytosol.

For comparison, ADPGlc levels were also analysed in the different fractions obtained after non-aqueous density fractionation of material from growing potato tubers (Fig. 5D). The overall level of ADPGlc in growing potato tubers was 20-fold lower than in wild-type barley endosperm and 4-fold lower than in the *Riso16* mutant lacking cytosolic AGPase (Table 2). In contrast to barley endosperm, almost all of the ADPGlc in growing potato tubers (>97%) was located in the plastid, whereas there was only a very minor amount in the cytosol (<3%). The very low amount of ADPGlc found in

the cytosol of growing tubers (~2% of the total, or 0.4  $\mu$ M) is possibly due to a small percentage of ADPGlc leaking out of the plastid. A comparison between ADPGlc (0.4  $\mu$ M) and UDPGlc (571  $\mu$ M; see Tiessen *et al.*, 2002) concentrations in the cytosol of growing tubers suggests that sucrose synthase is almost exclusively involved in UDPGlc synthesis *in vivo*, and that ADPGlc is at its best only a very minor by-product of sucrose synthase activity under these conditions. In addition to this, the estimated concentration of ADPGlc in the cytosol of growing potato tubers (~0.4  $\mu$ M) was 500 times lower than that in the cytosol of barley endosperm (~236–268  $\mu$ M), which is consistent with a very minor role, if any, for ADPGlc in the cytosol of growing tubers (Tables 1, 2). This is in agreement with the classical pathway of starch synthesis, involving ADPGlc synthesis in the plastid rather than the cytosol (Fig 1A). It also shows that the recently proposed new pathway of starch synthesis, involving synthesis of ADPGlc in the cytosol by sucrose synthase (Baroja-Fernandez *et al.*, 2004), is unlikely to operate in growing potato tubers.

#### Calculation of *in vivo* mass–action ratios for individual steps in the pathway from sucrose to starch to identify reversible and irreversible reactions in barley endosperm

Irreversible and reversible steps can be identified by measuring the *in vivo* concentrations of all the metabolites in the pathway. This allows the mass–action ratio (the ratio between the *in vivo* concentrations of the products and the substrates) to be calculated for every reaction. These can be compared with the respective equilibrium constants ( $K_{eq}$ , the ratio between the products and substrates when the reaction is at thermodynamic equilibrium and net flux is zero) to reveal how far each reaction is displaced from equilibrium. Since the reported values for  $K_{eq}$  can vary dependent on the pH and the ionic conditions, small differences between the *in vivo* mass–action ratio and its  $K_{eq}$  should not be overinterpreted. In general, a reaction will be regarded as irreversible when the mass–action ratio is displaced from its  $K_{eq}$  by a factor of >10.

To calculate the *in vivo* mass–action ratios of all steps between sucrose and starch, subcellular metabolite concentrations were used as documented in Table 1. The estimated *in vivo* mass–action ratios for developing barley endosperm are summarized in Table 3 and compared with the respective data for potato tubers from the literature and the theoretical equilibrium constants. Inspection of Table 3 shows that the *in vivo* mass–action ratios for the constituent enzymes of the pathways of sucrose degradation, starch synthesis, and glycolysis in barley endosperm largely resemble those calculated earlier for potato tubers (Farre *et al.*, 2001; Tiessen *et al.*, 2002), leaf material (Stitt *et al.*, 1982, 1989), and phloem sap (Geigenberger *et al.*, 1993). The *in vivo* mass–action ratios of the reactions catalysed by sucrose synthase, UGPase, phosphoglucoseisomerase, and PGM, and the transport exchange catalysed by the Glc6P/Pi transporter differed from their respective  $K_{eq}$  by a factor of <10, indicating readily reversible reactions *in vivo*. In

**Table 3.** Estimation of *in vivo* molar mass–action ratios for different metabolic reactions in cytosol and plastids of barley endosperm (14 DAF)

The values of the molar mass–action ratios were calculated using the mean metabolite concentrations from Table 1 and the equations given in the present table. The respective values determined in growing potato tubers, as well as the theoretical  $K_{eq}$  for each reaction step is shown for comparison (see Tiessen *et al.*, 2002).

Reaction	<i>In vivo</i> molar mass action ratio		Theoretical $K_{eq}$	Equations used for calculation
	Barley endosperm	Potato tuber		
SuSy	0.076	0.181	0.15	$\frac{[Fru] \times [UDPGlc]}{[Suc] \times [UDP]}$
UGPase	0.413	1.48	3.2	$\frac{[Glc1P] \times [UTP]}{[UDPGlc] \times [PPi]}$
Fructokinase	<b>0.022</b>	<b>0.032</b>	851	$\frac{[Fru6P] \times [UDP]}{[Fru] \times [UTP]}$
PGL	5.231	3.47	2	$\frac{[Glc6P]}{[Fru6P]}$
PGM	0.060	0.084	0.053	$\frac{[Glc1P]}{[Glc6P]}$
PGM (pl)	0.073	0.046	0.053	$\frac{[Glc1P]}{[Glc6P]}$
AGPase	1,003	ND	1	$\frac{[ADPGlc] \times [PPi]}{[Glc1P] \times [ATP]}$
AGPase (pl)	0.592	<b>0.016</b>	1	$\frac{[ADPGlc] \times [PPi]}{[Glc1P] \times [ATP]}$
ADPGlc/ADP transporter	<b>0.049</b>	ND	1	$\frac{[ADPGlc]_{pl} \times [ADP]_{ct}}{[ADP]_{pl} \times [ADPGlc]_{ct}}$
Glc6P/Pi transporter	0.579	2.04	1	$\frac{[Glc6P]_{pl} \times [Pi]_{ct}}{[Pi]_{pl} \times [Glc6P]_{ct}}$
PPDK (pl)	0.002	ND	0.005	$\frac{[PEP] \times [AMP] \times [PPi]}{[Pyr] \times [ATP] \times [Pi]}$
PFK	<b>0.038</b>	ND	308	$\frac{[Fru1,6bP] \times [ADP]}{[Fru6P] \times [ATP]}$
PK	<b>6.247</b>	ND	319 240	$\frac{[Pyr] \times [ATP]}{[PEP] \times [ADP]}$
PK (pl)	<b>0.875</b>	ND	319 240	$\frac{[Pyr] \times [ATP]}{[PEP] \times [ADP]}$
PPase	<b>2.899</b>	ND	1000	$\frac{[Pi] \times [Pi]}{[PPi]}$
PPase (pl)	<b>1.162</b>	<b>0.323</b>	1000	$\frac{[Pi] \times [Pi]}{[PPi]}$
ATPase	<b>0.002</b>	ND	222 001	$\frac{[ADP] \times [Pi]}{[ATP]}$
ATPase (pl)	<b>0.016</b>	ND	222 001	$\frac{[ADP] \times [Pi]}{[ATP]}$

Values that are displaced >10-fold from their respective  $K_{eq}$  pinpoint irreversible reactions and are indicated in bold. pl, plastid.

contrast to this, the mass–action ratios of fructokinase, phosphofructokinase, pyruvate kinase, inorganic pyrophosphatase, and ATPase were displaced from their  $K_{eq}$  by a factor of >10, indicating irreversible reactions *in vivo*.

However, the data for barley endosperm differed in two important aspects from those for potato and other tissues (Table 3). First, in barley, the mass–action ratio for the reaction catalysed by AGPase was close to its  $K_{eq}$  (1.0), indicating that the AGPase in both the cytosol (1.003) and plastid (0.592) catalyses readily reversible reactions *in vivo*. This is in contrast to potato tubers, where the plastidial AGPase is displaced from its equilibrium by two orders of magnitude (0.016), indicating an irreversible reaction *in vivo* (see Tiessen *et al.*, 2002). In general, AGPase can be rendered irreversible *in vivo* in many tissues including potato tubers by the efficient removal of one of its product, PPi, by high activities of inorganic pyrophosphatase in the plastid. Obviously, removal of plastidial PPi is less effective in barley endosperm compared with potato tubers. Indeed, plastidial PPi concentrations were almost 10-fold higher in barley endosperm (18  $\mu$ M; see Table 1) than in potato tubers (2.3  $\mu$ M; see Tiessen *et al.*, 2002).

A second important aspect of the data presented in Table 3 concerns the transport of ADPGlc into the plastid. This is

a specific feature of cereal endosperm metabolism and is absent in potato tubers and other dicot tissues. The wild-type barley *in vivo* mass–action ratio of the exchange catalysed by the ADPGlc/ADP transporter was displaced by more than one magnitude from its  $K_{eq}$ , indicating an effectively irreversible reaction *in vivo*. This provides evidence that the ADPGlc transport step in the pathway of starch synthesis in cereal endosperm is a potentially important site for regulation. This is in contrast to potato tubers, where neither the Glc6P/Pi nor the ATP/ADP exchange is significantly displaced from equilibrium (Farre *et al.*, 2001; Tiessen *et al.*, 2002).

## Discussion

Despite the central importance of metabolic compartmentation in plant cells, there have been only a few studies exploring this issue. Most of these studies were focused on photosynthetic leaves (Gerhardt *et al.*, 1987; Riens *et al.*, 1991; Leidreiter *et al.*, 1995; Fettke *et al.*, 2005; Geigenberger *et al.*, 2011), whereas analysis of non-photosynthetic tissues was mainly focused on potato tubers (Farre *et al.*, 2001; Tiessen *et al.*, 2002). In the present study, a protocol for NAF of barley endosperm tissue is described. By using

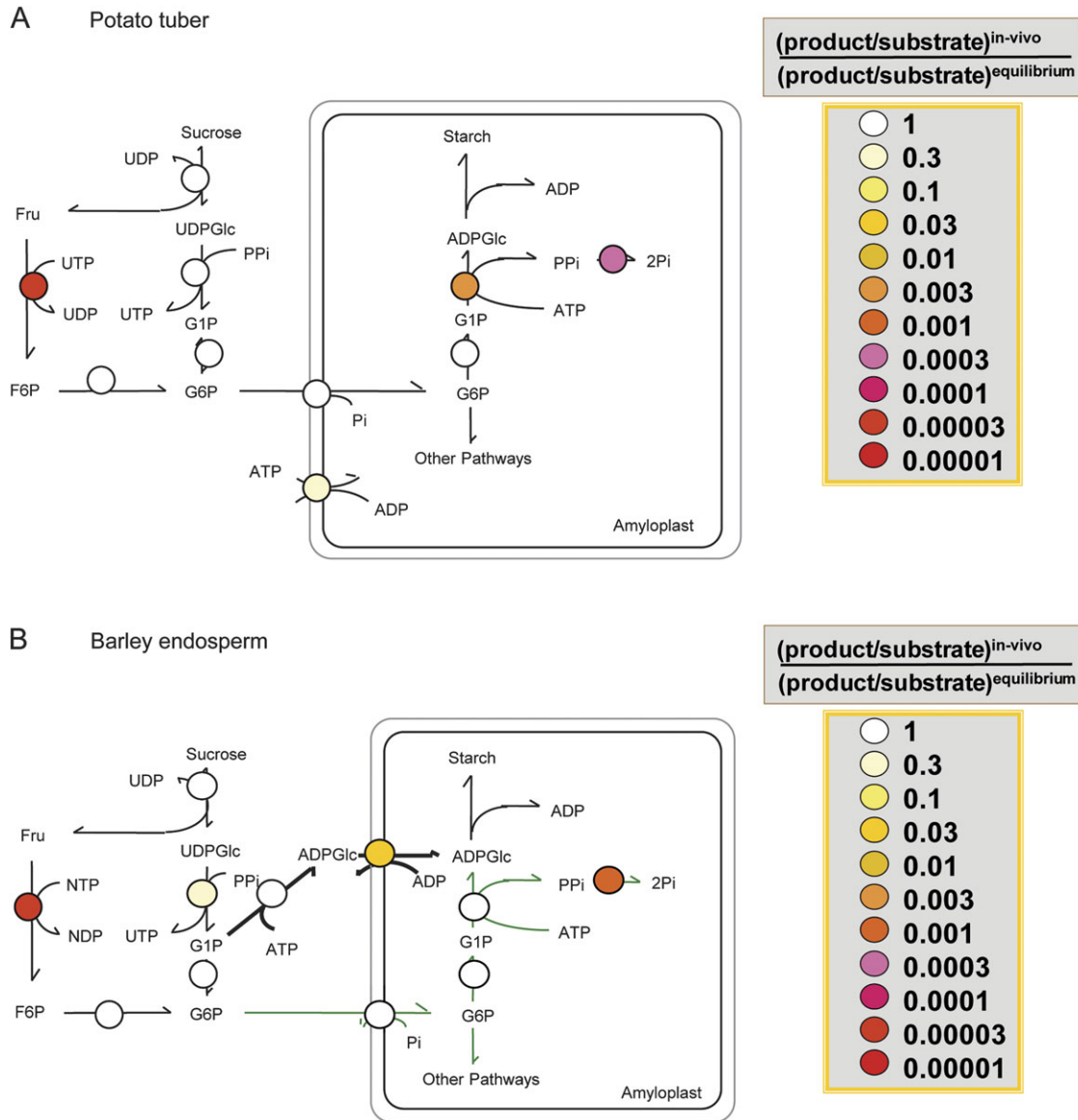


**Fig. 5.** Comparison of the thermodynamic structure of the pathway of sucrose to starch in growing potato tubers (A) and developing barley endosperm (B). For each step in the pathway, thermodynamic properties are indicated using a false-colour code. False-colour symbols represent the ratio  $T/K_{eq}$  showing how far each reaction is displaced from equilibrium, with  $T$  being the ratio between the *in vivo* subcellular concentrations of the products and the substrates of each reaction. Data are taken from Table 3 (see also Geigenberger *et al.*, 2004 for potato tubers). For designation of the different steps, see Fig. 1. In general, a reaction is regarded as irreversible when the mass-action ratio is displaced from its  $K_{eq}$  by a factor  $>10$ .

this method, it was possible to determine the *in vivo* subcellular distribution between the cytosol and plastid of the levels and concentrations of metabolites involved in sucrose degradation, starch synthesis, and respiration in the developing endosperm. Although Liu and Shannon (1981a, b) reported on an NAF method for isolation of maize endosperm starch granules and their associated metabolites, their method used solvents that lead to inactivation of enzyme activities, thus preventing a comparison with the distribution of marker enzymes (Shannon *et al.*, 1998).

Microscopic analysis shows that developing barley endosperm cells consist of two major subcellular compartments, plastids and cytosol, comprising  $\sim 50.5\%$  and  $49.5\%$

of the total cell volume, respectively (Fig. 2). This differs from potato tubers and leaves where three major compartments can be detected, plastids, cytosol, and vacuoles, comprising 16–19, 4–7, and 73–79% of the total cell volume, respectively (see Farre *et al.*, 2001). Consistent with this, no enrichment of the vacuolar marker relative to the cytosolic markers was obtained in the non-aqueous fractions of barley endosperm (Fig. 3), and the pellet fraction, which is usually enriched in vacuolar particles in potato tuber and leaf gradients, was essentially free of subcellular particles in the barley gradients (Fig. 4). The method described herein is therefore applicable to determine subcellular metabolite concentrations in the cytosol and plastids of developing

barley endosperm. The failure to resolve the vacuolar compartment from the cytosolic compartment in the non-aqueous barley gradients is probably due to the fact that barley seed vacuoles are very small and have a different composition from those in other plant tissues. Similarly, all previous non-aqueous fractionation experiments failed to discriminate the mitochondrial from other compartments of plant tissues (see above).

*The subcellular distribution of ADPGlc in cereal endosperm differs from that in potato tubers and is significantly modified by inactivation of the brittle1- homologous ADPGlc/ADP transporter*

In developing barley endosperm, the immediate precursor of starch synthesis, ADPGlc, was mainly located in the cytosol (80–90%), whereas in growing potato tubers, ADPGlc was almost exclusively located in the plastid (>97%), reflecting the different subcellular compartmentation of AGPase in these tissues (see Tables 1, 2). The subcellular concentrations of ADPGlc were also analysed in low-starch barley mutants which are defective in genes encoding cytosolic AGPase (*Riso16*; Johnson *et al.*, 2003) and the ADPGlc/ADP transporter at the plastid envelope (*Riso13*; Patron *et al.*, 2004). Inactivation of cytosolic AGPase in *Riso16* endosperm led to a strong decrease in ADPGlc levels in both the cytosol and plastid. In contrast, inactivation of the ADPGlc/ADP transporter led to a large shift in the intracellular distribution of ADPGlc, being strongly increased in the cytosol (> 20-fold), while being decreased to values near the detection limit in the plastid (Table 2). These results are consistent with previous studies on the aqueous fractionation of enzyme activities that suggested that most of the ADPGlc in barley endosperm is formed in the cytosol and requires transport into the plastid to serve as the immediate precursor of starch synthesis (for a review, see James *et al.*, 2003). However, in the *Riso16* mutant, a residual AGPase activity of ~20% of the wild-type level could be measured (data not shown), confirming previous data from Johnson *et al.* (2003) and indicating that a significant amount of AGPase remained in the plastid of this mutant.

The relatively high concentrations of ADPGlc measured in the cytosol of wild-type barley endosperm (268  $\mu\text{M}$ ; see Table 1) are reflected in the relatively high  $K_m$  of the ADPGlc/ADP transporter for ADPGlc (850  $\mu\text{M}$ ; see Kirchberger *et al.*, 2007). This means that changes in the ADPGlc concentration in the cytosol will directly affect the activity of the ADPGlc transporter at the plastid envelope. When the ADPGlc/ADP transporter was inactivated in *Riso13*, the ADPGlc concentration in the cytosol increased to >4000  $\mu\text{M}$ , whereas inactivation of cytosolic AGPase in *Riso16* led to opposite changes (see Table 2). This shows the dynamic range of cytosolic ADPGlc concentrations in barley endosperm (60–4000  $\mu\text{M}$ ), which are mainly determined by the balance between cytosolic AGPase and ADPGlc/ADP transporter activities. The range of ADPGlc concentrations in the plastid is much smaller (1–70  $\mu\text{M}$ ) and mainly determined by the ADPGlc/ADP transport activity (Table 2).

*The thermodynamic structure of the pathway of starch synthesis in barley endosperm is different from that in potato tubers and most other plant tissues*

A further important aspect in understanding the regulation of the pathway of starch synthesis is to identify which reactions are readily reversible and which are effectively irreversible *in vivo*. This has important implications for regulation, since the closer the reaction is to equilibrium, the smaller are the changes of effectors that are needed to produce a given change of flux (Stitt *et al.*, 2010). Conversely, irreversible reactions have often been found to be targets of regulatory mechanisms and signals, which allow changes in metabolic fluxes independently of changes in substrate concentrations (Stitt *et al.*, 2010).

In potato tubers, systematic analyses of the mass-action ratios of each step in the pathway of starch synthesis pinpointed fructokinase in the cytosol as well as AGPase and inorganic pyrophosphatase in the plastid as catalysing irreversible reactions *in vivo* (Geigenberger *et al.*, 2004; see Fig. 5A). The results of the present study show that the thermodynamic structure of the pathway of starch synthesis in developing barley endosperm is different from that in potato tubers with respect to the free energy change and reversibility of the reactions catalysed by (i) AGPase and (ii) the carbon transporter at the amyloplast envelope (compare Fig. 5A and 5B).

*The major form of AGPase in developing barley endosperm catalyses a readily reversible reaction in the cytosol with important implications for regulation*

As shown in Fig. 5, AGPase catalyses a near-equilibrium and readily reversible reaction *in vivo* in the cytosol. Direct evidence is provided by comparing the estimated *in vivo* mass-action ratios with the theoretical  $K_{eq}$  of the reaction (Table 3). Comparison of the cytosolic concentrations of the reaction partners of AGPase in barley endosperm (Table 1) with the respective  $K_m$  values of AGPase reported for the purified barley enzyme (Doan *et al.*, 1999) provides another line of evidence that AGPase will be active in both reaction directions *in vivo*. The *in vivo* flux catalysed by cytosolic AGPase will therefore depend directly on the cytosolic concentrations of Glc1P and ATP provided by sucrose degradation and respiration, respectively, and on the rate at which ADPGlc and PPI are used by the ADPGlc/ADP transporter at the amyloplast envelope and different PPI-dependent reactions in the cytosol (such as UGPase, PFP, or PPI-dependent proton pumps), respectively. This opens up new strategies for genetic engineering to alter carbon partitioning and the rate of starch synthesis in cereal endosperm. For example, overexpression of inorganic pyrophosphatase to decrease PPI levels in the cytosol might increase provision of ADPGlc for starch synthesis, unless provision of Glc1P via PPI-dependent UGPase is not compromised. More studies are needed to explore the potential of manipulating the concentrations of the reaction partners of AGPase to increase partitioning into starch.

The reversibility of AGPase makes this enzyme more sensitive to changes in the level of substrates to produce a given change in flux. This is consistent with the major form of AGPase from cereal endosperm displaying much weaker regulatory properties than its counterpart in potato tubers or leaves, which catalyse irreversible reactions. First, cereal endosperm AGPase has much weaker allosteric properties, being essentially insensitive to allosteric activation by 3-phosphoglyceric acid or inhibition by Pi in barley (Doan *et al.*, 1999) and wheat endosperm (Tetlow *et al.*, 2004a). Secondly, the major form of AGPase in cereal endosperm is missing the regulatory Cys82 in its small subunits which is involved in post-translational redox modification of the enzyme in leaves and potato tubers in response to sucrose supply (Tiessen *et al.*, 2002; Hendriks *et al.*, 2003). This would imply that the majority of AGPase in cereal endosperm is insensitive to post-translational regulation by sucrose signals. However, direct evidence is lacking at the moment to exclude that redox regulation of cytosolic AGPase in barley endosperm might operate via different cysteine residues.

*The reversibility of AGPase in the plastid has important implications for pathway regulation and biotechnological approaches in cereal endosperm*

The finding that barley endosperm AGPase catalyses a readily reversible reaction in the plastid is unexpected. In most other tissues, including leaves and potato tubers, plastidial AGPase is far displaced from equilibrium due to removal of PPI by inorganic pyrophosphatase (Gross and apRees, 1986; Weiner *et al.*, 1987). Obviously, removal of plastidial PPI is less efficient in barley endosperm than in potato tubers, although inorganic pyrophosphatase activity is relatively high ( $300 \mu\text{mol min}^{-1} \text{g DW}^{-1}$ , data not shown). Consistent with this, PPI concentrations are much higher in the plastids of barley than in those of potato tubers. The reversibility of the plastidial AGPase in barley endosperm suggests that this enzyme is also able to catalyse the reverse reaction *in vivo*, the conversion of ADPGlc and PPI to Glc1P and ATP. Generation of Glc1P and ATP would be important to feed biosynthetic processes other than starch synthesis (i.e. amino acid synthesis) in the plastid. One of the substrates for the reverse reaction of AGPase, ADPGlc, is imported from the cytosol, while PPI could be generated by plastidial PPDK activity as suggested by Hennen-Bierwagen *et al.* (2009). However, the sub-cellular distribution of PPDK in cereal endosperm has not been fully clarified yet. Therefore, PPDK may also change carbon partitioning in the cytosol by modifying cytosolic PPI and ATP levels as suggested by Mechin *et al.* (2007).

The present data indicate that plastidial PPDK catalyses a readily reversible reaction *in vivo*, with the reaction being slightly shifted in the direction of PPI formation (Table 3). Both AGPase and PPDK have been found to be associated in multienzyme complexes, together with other starch biosynthetic enzymes in cereal endosperm (Hennen-Bierwagen *et al.*, 2009). Due to the reversibility of AGPase, changes in the plastidial concentrations of ADPGlc, PPI, Glc1P, and ATP

will affect the reaction equilibrium and hence the partitioning of carbon between starch and other biosynthetic pathways. Although overexpression of *Escherichia coli* pyrophosphatase in the plastid had no effect on carbon fluxes in potato tubers (Farre *et al.*, 2006), a similar approach in cereal endosperm might shift the reversible AGPase reaction in the direction of PPI and ADPGlc formation, supporting starch biosynthesis at the expense of amino acid synthesis in the plastid. Interestingly, knock-out of cytosolic AGPase in the *Riso16* mutant led to a strong decrease in plastidial ADPGlc levels (Table 2) and to low levels of amino acids in the developing endosperm (Faix *et al.*, 2011). The reversibility of the plastidial AGPase reaction might also explain some pleiotropic effects of the *brittle1* mutants, which are blocked in transport and subsequent delivery of ADPGlc to provide carbon (Glc1P) and energy (ATP) required for other plastidial pathways beside starch. Further studies are required to investigate the role of the reversibility of cereal endosperm AGPase in regulating the partitioning between starch and amino acid synthesis in the plastid. Since the malting industry is interested in manipulating the starch/protein ratio for beer production, this also has biotechnological implications.

*The ADPGlc/ADP transporter at the plastid envelope catalyses an irreversible reaction in barley endosperm and is subject to regulatory signals*

In contrast to AGPase, the ADPGlc/ADP transporter at the plastid envelope has been found to be strongly displaced from equilibrium (Table 3; Fig. 5). It is therefore very likely that this transporter is subject to regulatory mechanisms and signals. Intriguingly, recent proteomic approaches identified the wheat *brittle1* ADPGlc/ADP transporter as a potential thioredoxin target (Balmer *et al.*, 2006). *Brittle1* homologues possess several conserved cysteines, and the transport protein from maize has been found to be inhibited by diamine and reversibly activated by DTT (Kirchberger *et al.*, 2007). This provides evidence that the ADPGlc/ADP transporter in cereal endosperm is subject to post-translational redox regulation. The components of a complete ferredoxin/thioredoxin system have been identified recently in amyloplasts isolated from wheat endosperm (Balmer *et al.*, 2006). In amyloplasts, ferredoxin is most probably reduced by metabolically generated NADPH via ferredoxin-NADP reductase (Balmer *et al.*, 2006). Alternatively, NADPH may lead to reductive activation of the ADPGlc/ADP transporter via NADP-thioredoxin reductase C, which includes a Trx domain on the same polypeptide and has been found to be located in the plastid (Michalska *et al.*, 2009). Increased NADPH/NADP ratios may act as a sucrose signal, leading to a stimulation of starch synthesis by redox activation of ADPGlc transport into plastids. More studies are needed to dissect this putative signalling pathway and to resolve the thiol–disulphide network and its target proteins in cereal endosperm *in vivo*.

## Conclusions

In this report, an NAF technique was applied to analyse subcellular metabolite concentrations in the developing

barley endosperm. The subcellular distribution of ADPGlc and the thermodynamic structure of the pathway from sucrose to starch have been found to be different from those in most other tissues. AGPase catalyses a readily reversible reaction, both in the cytosol and in the plastid, which has important implications for the regulation of carbon partitioning between different biosynthetic pathways in response to changes in supply and demand. Since the ADPGlc/ADP transporter was found to catalyse an irreversible reaction, this transport step between the cytosol and plastid is pinpointed as a potential regulatory site and target of external signals. More work will be needed to resolve this regulatory network in cereal endosperm fully and to assess the biotechnological implications for crop improvement.

## Acknowledgements

This work was supported by the Bundesministerium für Bildung und Forschung (GABI-Future project SysSeed, grant 0315044C to PG, AN, BF, HW, and WW) and the Deutsche Forschungsgemeinschaft (project Ge 878/5-1 to PG). AT is grateful to the Sonderforschungsbereich TR1 for kindly providing a travel grant to support his stay at the Department of Biology I at the LMU Munich. We are grateful to Joost van Dongen and Sonja Reiland (MPI-MP Golm) for performing preliminary analyses.

## References

- Angeles-Nuñez JG, Tiessen A.** 2010. Arabidopsis sucrose synthase 2 and 3 modulate metabolic homeostasis and direct carbon towards starch synthesis in developing seeds. *Planta* **232**, 701–718.
- Avigad G.** 1982. Sucrose and other disaccharides. In: Loewus FA, Tanner W, eds. *Encyclopedia of plant physiology*. Berlin: Springer-Verlag, 217–347.
- Balmer Y, Vensel W, Cai N, Manieri W, Schurmann P, Hurkman W, Buchanan B.** 2006. A complete ferredoxin/thioredoxin system regulates fundamental processes in amyloplasts. *Proceedings of the National Academy of Sciences, USA* **103**, 2988–2993.
- Baroja-Fernandez E, Munoz FJ, Zanduetta-Criado A, Moran-Zorzano MT, Viale AM, Alonso-Casajús N, Pozueta-Romero J.** 2004. Most of ADP-glucose linked to starch biosynthesis occurs outside the chloroplast in source leaves. *Proceedings of the National Academy of Sciences, USA* **101**, 13080–13085.
- Bowsher CG, Scrase-Field EFAL, Esposito S, Emes MJ, Tetlow IJ.** 2007. Characterization of ADP-glucose transport across the cereal endosperm amyloplast envelope. *Journal of Experimental Botany* **58**, 1321–1332.
- Bradford MM.** 1976. Rapid and sensitive method for quantitation of microgram quantities of protein utilizing the principle of protein–dye binding. *Analytical Biochemistry* **72**, 248–254.
- Burton RA, Jenner H, Carrangis L, et al.** 2002. Starch granule initiation and growth are altered in barley mutants that lack isoamylase activity. *The Plant Journal* **31**, 97–112.
- Delesse MA.** 1847. Procédé mécanique pour déterminer la composition des roches. *Comptes Rendus de l'Académie des Sciences, Paris* **25**, 544.
- Doan DNP, Rudi H, Olsen O-A.** 1999. The allosterically unregulated isoform of ADP-glucose pyrophosphorylase from barley endosperm is the most likely source of ADP-glucose incorporated into endosperm starch. *Plant Physiology* **121**, 965–975.
- Faix B, Radchuk V, Nerlich A, et al.** 2011. Barley grains, deficient in cytosolic small subunit of ADP-glucose pyrophosphorylase, reveal coordinate adjustment of C: N metabolism mediated by an overlapping metabolic–hormonal control. *The Plant Journal* in press.
- FAO.** 2003. *Diet, nutrition and the prevention of chronic diseases*. Report of a Joint WHO/FAO Expert Consultation. Geneva: WHO/FAO.
- Farre EM, Tech S, Trethewey RN, Fernie AR, Willmitzer L.** 2006. Subcellular pyrophosphate metabolism in developing tubers of potato (*Solanum tuberosum*). *Plant Molecular Biology* **62**, 165–179.
- Farre EM, Tiessen A, Roessner U, Geigenberger P, Trethewey RN, Willmitzer L.** 2001. Analysis of the compartmentation of glycolytic intermediates, nucleotides, sugars, amino acids and sugar alcohols in potato tubers using a non-aqueous fractionation method. *Plant Physiology* **127**, 685–700.
- Fettke J, Eckermann N, Tiessen A, Geigenberger P, Steup M.** 2005. Identification, subcellular localisation and biochemical characterization of water-soluble heteroglycans (SHG) in leaves of *Arabidopsis thaliana* L.: distinct SHG reside in the cytosol and in the apoplast. *The Plant Journal* **43**, 568–585.
- Geigenberger P.** 2011. Regulation of starch biosynthesis in response to a fluctuating environment. *Plant Physiology* **155**, 1566–1577.
- Geigenberger P, Fernie AR.** 2006. Starch synthesis in the potato tuber. In: Hui YH, Corke H, DeLeyn I, Nip W-K, Cross N, eds. *Food biochemistry and food processing*. Ames, IA: Blackwell Publishing, 253–270.
- Geigenberger P, Langenberger S, Wilke I, Heineke D, Heldt HW, Stitt M.** 1993. Sucrose is metabolised by sucrose synthase and glycolysis within the phloem complex of *Ricinus communis* L. seedlings. *Planta* **190**, 446–453.
- Geigenberger P, Reimholz R, Geiger M, Merlo L, Canale V, Stitt M.** 1997. Regulation of sucrose and starch metabolism in potato tubers in response to short-term water deficit. *Planta* **201**, 502–518.
- Geigenberger P, Stamme C, Tjaden J, Schulz A, Quick PW, Betsche T, Kersting HJ, Neuhaus HE.** 2001. Tuber physiology and properties of starch from tubers of transgenic potato plants with altered plastidic adenylate transporter activity. *Plant Physiology* **125**, 1667–1678.
- Geigenberger P, Stitt M, Fernie AR.** 2004. Metabolic control analysis and regulation of the conversion of sucrose to starch in growing potato tubers. *Plant, Cell and Environment* **27**, 655–673.
- Geigenberger P, Tiessen A, Meurer J.** 2011. Use of non-aqueous fractionation and metabolomics to study chloroplast function in *Arabidopsis*. *Methods in Molecular Biology* **775**, 135–160.
- Gerhardt R, Heldt HW.** 1984. Measurement of subcellular metabolite levels in leaves by fractionation of freeze-stopped material in nonaqueous media. *Plant Physiology* **75**, 542–547.

- Gerhardt R, Stitt M, Heldt HW.** 1987. Subcellular metabolite levels in spinach leaves. *Plant Physiology* **83**, 399–407.
- Gross P, ap Rees T.** 1986. Alkaline inorganic pyrophosphatase and starch synthesis in amyloplasts. *Planta* **167**, 140–145.
- Gubatz S, Dercksen VJ, Brüß C, Weschke W, Wobus U.** 2007. Analysis of barley (*Hordeum vulgare*) grain development using three-dimensional digital models. *The Plant Journal* **52**, 779–790.
- Hannah LC, James M.** 2008. The complexities of starch biosynthesis in cereal endosperms. *Current Opinion in Biotechnology* **19**, 160–165.
- Heineke D, Lohaus G, Winter H.** 1997. Compartmentation of C/N metabolism. In: Foyer CH, Quick WP, eds. *A molecular approach to primary metabolism in higher plants*. London: Taylor & Francis, 205–217.
- Hendriks JHM, Kolbe A, Gibon Y, Stitt M, Geigenberger P.** 2003. ADP-glucose pyrophosphorylase is activated by posttranslational redox-modification in response to light and to sugars in leaves of *Arabidopsis* and other plant species. *Plant Physiology* **133**, 838–849.
- Hennen-Bierwagen TA, Liu F, Marsh RS, Kim S, Gan Q, Tetlow IJ, Emes MJ, James MG, Myers AM.** 2008. Starch biosynthetic enzymes from developing maize endosperm associate in multisubunit complexes. *Plant Physiology* **146**, 1892–1908.
- Hennen-Bierwagen TA, Lin Q, Grimaud F, Planchot V, Keeling PL, James MG, Myers AM.** 2009. Proteins from multiple metabolic pathways associate with starch biosynthetic enzymes in high molecular weight complexes: a model for regulation of carbon allocation in maize amyloplasts. *Plant Physiology* **149**, 1541–1559.
- James MG, Denyer K, Myers AM.** 2003. Starch synthesis in the cereal endosperm. *Current Opinion in Plant Biology* **6**, 215–222.
- Jenner CF, Denyer K, Hawker JS.** 1994. Caution on the use of the generally accepted methanol precipitation technique for the assay of soluble starch synthase in crude extracts of plant tissues. *Australian Journal of Plant Physiology* **21**, 17–22.
- Jeon JS, Ryoo N, Hahn TR, Walia H, Nakamura Y.** 2010. Starch biosynthesis in cereal endosperm. *Plant Physiology and Biochemistry* **48**, 383–392.
- Johnson PE, Patron NJ, Bottrill AR, Dinges JR, Fahy BF, Parker ML, Waite DN, Denyer K.** 2003. A low-starch barley mutant, Risø 16, lacking the cytosolic small subunit of ADP-glucose pyrophosphorylase, reveals the importance of the cytosolic isoforms and the identity of the plastidial small subunit. *Plant Physiology* **131**, 684–696.
- Kammerer B, Fisher K, Hilpert B, Schuber S, Gutensohn M, Weber A, Flügge U-I.** 1998. Molecular characterisation of a carbon transporter in plastids from heterotrophic tissues: the glucose 6-phosphate antiporter. *The Plant Cell* **10**, 105–117.
- Kirchberger S, Leroch M, Huynen M, Wahl M, Neuhaus HE, Tjaden J.** 2007. Molecular and biochemical analysis of the plastidic ADP-glucose transporter (ZmBT1) from *Zea mays*. *Journal of Biological Chemistry* **282**, 22481–22491.
- Leidreiter K, Kruse A, Heineke D, Robinson DG, Heldt HW.** 1995. Subcellular volumes and metabolic concentrations in potato (*Solanum tuberosum* cv. Desiree) leaves. *Botanica Acta* **108**, 439–444.
- Liu TL, Shannon JC.** 1981a. A non-aqueous procedure for isolating starch granules with associated metabolites from maize (*Zea mays* L.) endosperm. *Plant Physiology* **67**, 518–524.
- Liu T-TY, Shannon JC.** 1981b. Measurement of metabolites associated with nonaqueously isolated starch granules from immature *Zea mays* L. endosperm. *Plant Physiology* **67**, 525–529.
- Liu F, Makhmoudova A, Lee EA, Wait R, Emes MJ, Tetlow IJ.** 2009. The amylose extender mutant of maize conditions novel protein–protein interactions between starch biosynthetic enzymes in amyloplasts. *Journal of Experimental Botany* **60**, 4423–4440.
- Mangelsdorf PC, Jones DF.** 1926. The expression of mendelian factors in the gametophyte of maize. *Genetics* **11**, 423–455.
- Mechin V, Thevenot C, Le Guilloux M, Prioul JL, Damerval C.** 2007. Developmental analysis of maize endosperm proteome suggests a pivotal role for pyruvate orthophosphate dikinase. *Plant Physiology* **143**, 1203–1219.
- Merlo L, Geigenberger P, Hajirezaei M, Stitt M.** 1993. Changes of carbohydrates, metabolites and enzyme activities in potato tubers during development, and within a single tuber along a stolon–apex gradient. *Journal of Plant Physiology* **142**, 392–402.
- Michalska J, Zauber H, Buchanan BB, Cejudo FJ, Geigenberger P.** 2009. NTRC links built-in thioredoxin to light and sucrose in regulating starch synthesis in chloroplasts and amyloplasts. *Proceedings of the National Academy of Sciences, USA* **106**, 9908–9913.
- Patron NJ, Greber B, Fahy BF, Laurie DA, Parker ML, Denyer K.** 2004. The *lys5* mutations of barley reveal the nature and importance of plastidial ADP-Glc transporters for starch synthesis in cereal endosperm. *Plant Physiology* **135**, 2088–2097.
- Riens B, Lohaus G, Heineke D, Heldt HW.** 1991. Amino acid and sucrose content determined in the cytosolic, chloroplastic, and vacuolar compartments and in the phloem sap of spinach leaves. *Plant Physiology* **97**, 227–233.
- Shannon JC, Pien F-M, Cao H, Liu K-C.** 1998. Brittle-1, an adenylate translocator, facilitates transfer of extra plastidial synthesised ADP-glucose into amyloplasts of maize endosperms. *Plant Physiology* **117**, 1235–1252.
- Smith AM.** 2008. Prospects for increasing starch and sucrose yields for bioethanol production. *The Plant Journal* **54**, 546–558.
- Stitt M, Lilley RM, Gerhardt R, Heldt HW.** 1989. Metabolite levels in specific cells and subcellular compartments of plant leaves. *Methods in Enzymology* **174**, 518–550.
- Stitt M, Lilley RM, Heldt HW.** 1982. Adenine nucleotide levels in the cytosol, chloroplasts, and mitochondria of wheat leaf protoplasts. *Plant Physiology* **70**, 971–977.
- Stitt M, Sulpice R, Keurentjes J.** 2010. Metabolic networks: how to identify key components in the regulation of metabolism and growth? *Plant Physiology* **152**, 428–444.
- Sugiyama T.** 1973. Purification, molecular and catalytic properties of pyruvate phosphate dikinase from maize leaf. *Biochemistry* **12**, 2862–2868.
- Tetlow IJ, Beisel KG, Cameron S, Makhmoudova A, Liu F, Bresolin NS, Wait R, Morell MK, Emes MJ.** 2008. Analysis of protein complexes in wheat amyloplasts reveals functional interactions among starch biosynthetic enzymes. *Plant Physiology* **146**, 1878–1891.
- Tetlow IJ, Morell MK, Emes MJ.** 2004a. Recent developments in understanding the regulation of starch metabolism in higher plants. *Journal of Experimental Botany* **55**, 2131–2145.

- Tetlow IJ, Wait R, Lu Z, Akkasaeng R, Bowsher CG, Esposito S, Kosar-Hashemi B, Morell MK, Emes MJ.** 2004b. Protein phosphorylation in amyloplasts regulates starch branching enzyme activity and protein–protein interactions. *The Plant Cell* **16**, 694–708.
- Tiessen A.** 2000. Regulation of carbon metabolism in potato tubers in response to sink–source manipulations. *Diplomarbeit* Universität Heidelberg, Germany.
- Tiessen A, Hendriks JHM, Stitt M, Branscheid A, Gibon Y, Farre EM, Geigenberger P.** 2002. Starch synthesis in potato tubers is regulated by post-translational redox modification of ADP-glucose pyrophosphorylase: a novel regulatory mechanism linking starch synthesis to the sucrose supply. *The Plant Cell* **14**, 2191–2213.
- Trethewey RN, Geigenberger P, Riedel K, Hajirezaei M-R, Sonnewald U, Stitt M, Riesmeier JW, Willmitzer L.** 1998. Combined expression of glucokinase and invertase in potato tubers leads to a dramatic reduction in starch accumulation and a stimulation of glycolysis. *The Plant Journal* **15**, 109–118.
- Tjaden J, Möhlmann T, Kampfenkel K, Henrichs G, Neuhaus HE.** 1998. Altered plastidic ATP/ADP-transporter activity influences potato (*Solanum tuberosum* L.) tuber morphology, yield and composition of starch. *The Plant Journal* **16**, 531–540.
- Van Dongen JT, Roeb GW, Dautzenberg M, Froehlich A, Vigeolas H, Minchin PEH, Geigenberger P.** 2004. Phloem import and storage metabolism are highly coordinated by the low oxygen concentrations within developing wheat seeds. *Plant Physiology* **135**, 1809–1821.
- Weibel ER, Bolender RP.** 1973. Stereological techniques for electron microscopic morphometry. In: Hayat MA, ed. *Principles and techniques of electron microscopy, biological applications*. New York: P Van Nostrand Reinhold Company, 237–296.
- Weiner H, Stitt M, Heldt HW.** 1987. Sub-cellular compartmentation of pyrophosphate and alkaline pyrophosphatase in leaves. *Biochimica et Biophysica Acta* **893**, 13–21.
- Weschke W, Panitz R, Sauer N, Wang Q, Neubohn B, Weber H, Wobus U.** 2000. Sucrose transport into barley seeds: molecular characterization of two transporters and implications for seed development and starch accumulation. *The Plant Journal* **21**, 455–467.
- Winter H, Robinson DG, Heldt HW.** 1993. Sub-cellular volumes and metabolite concentrations in barley leaves. *Planta* **191**, 180–190.
- Zabalza A, van Dongen JT, Froehlich A, et al.** 2009. Regulation of respiration and fermentation to control the plant internal oxygen concentration. *Plant Physiology* **149**, 1087–1098.
- Zeeman SC, Kossmann J, Smith AM.** 2010. Starch: its metabolism, evolution, and biotechnological modification in plants. *Annual Review of Plant Biology* **61**, 209–234.